

PCCP

Accepted Manuscript



This is an Accepted Manuscript, which has been through the Royal Society of Chemistry peer review process and has been accepted for publication.

Accepted Manuscripts are published online shortly after acceptance, before technical editing, formatting and proof reading. Using this free service, authors can make their results available to the community, in citable form, before we publish the edited article. We will replace this Accepted Manuscript with the edited and formatted Advance Article as soon as it is available.

You can find more information about Accepted Manuscripts in the [Information for Authors](#).

Please note that technical editing may introduce minor changes to the text and/or graphics, which may alter content. The journal's standard [Terms & Conditions](#) and the [Ethical guidelines](#) still apply. In no event shall the Royal Society of Chemistry be held responsible for any errors or omissions in this Accepted Manuscript or any consequences arising from the use of any information it contains.



Physical Chemistry Chemical Physics

ARTICLE

Theoretical Prediction of Silicene; as New Candidate for the Anode of Lithium-Ion Batteries

Received 00th January 20xx,
Accepted 00th January 20xx

DOI: 10.1039/x0xx00000x

www.rsc.org/

S. M. Seyed-Talebi,^a I. Kazeminezhad^a and J. Beheshtian^b

Using density functional theory calculations, we determine the band structure and DOS of graphene and silicene supercell models. We also study adsorption mechanism of Li metal atom and Li-ion onto free-standing silicene (buckled, $\theta=101.7^\circ$) and compare the results with those of graphene. In contrast to graphene, interactions between Li metal atoms and Li-ions with silicene surface are quite strong due to its highly reactive buckled hexagonal structure. As a consequence of structural properties adsorption height, most stable adsorption site and energy barrier against Li diffusion are also discussed here to outline the prospects of using silicene in electronic devices such as Li ion batteries (LiBs), hydrogen storage and molecular machines. However, in most LiBs graphene layers are used as anode electrode. Here, it is shown that graphene has very limited Li storage capacity and low surface area than the silicene. As our models are in good agreement with previous predictions, this finding presents, a possible avenue for creating better anode material that can replace with graphene for higher capacity and better cycling performance of LiBs.

1 Introduction

Lithium (Li), the lightest metal (equivalent weight=6.94 g mol⁻¹, density= 0.53 g cm⁻³), is an ideal material for most consumer electronics. Lithium ions are slightly lower in energy density than lithium metals.¹ Because of the inherent instability of Lithium metal, especially during charging, Lithium-ion batteries are the choice in most rechargeable batteries.

Rechargeable lithium-ion batteries operate on the principle of storing and releasing lithium ions. When a battery is charging, ions move through an electrolyte from the cathode to the anode. Lithium ions insert themselves in the anode material by increasing the anode lithium storage capacity of the battery.

Graphite is the commercial anode material widely used for Li batteries because of its high efficiency and better cycle performance.² Therefore, the anode used in most Li-ion batteries is based on graphite carbon, which stores up to one Li ion for every six carbon atom between its graphene layers.³ Due to the limited capacity of graphite, the energy density of Li-ion battery cannot satisfy the requirements of portable electronic devices. Traditional intercalation graphite base anodes show low Li storage capacity (<372 mAh g⁻¹, LiC6) due to limited Li ion storage sites within the hexagonal carbon structure.^{3,4} Therefore, it is necessary to search new anode materials with high-rate capabilities and good performances. It has been shown that the capacity of current

battery anodes can be theoretically increased by replacing carbon materials with new anode materials such as silicone.⁵⁻⁸ Si-based anodes exhibits a theoretical capacity of ~4200 mAh g⁻¹ which is more than 10 times that of graphite anode ~370 mAh g⁻¹.^{9,10}

Up to now, the different adsorption mechanism of atoms and molecules onto graphene surface and doping effect on the adsorption capacity of graphene is frequently investigated¹¹⁻¹². Some experimental results have shown that graphene, a single atomic-layer thickness of graphite, can adsorb higher amounts of Li (e.g. specific capacity of ~540 mAh g⁻¹) than graphite¹³⁻¹⁵. Actually, besides graphene and its allotropes¹⁵⁻¹⁶, doped graphene sheets¹⁷⁻¹⁹ and more complex multi-component graphene base materials¹⁹⁻²¹ have also been explored as efficient anode materials with large capacity and high rate for lithium batteries.

Silicene, the silicon analogue of graphene, being of atomic thickness could serve as high-capacity host of Li in both cases of Li metal-based or Li-ion rechargeable batteries. The aim of this work is to study the essential differences between adsorption energy of Li atom and Li ion onto silicene and graphene surfaces. We focus on the interaction between a Li metal (or a Li-ion) and silicene surface in more details and compare our results with those of for graphene, which to the best of our knowledge has not been studied so far. We show that how the presence of silicene changes substantially lithium adsorption properties and consequently the capacity of current in the Li battery anodes. Improvements in anode materials have the potential of increasing the energy density. Therefore, the predictions in the present paper are important for Si-based anodes researches and provide physical insights about adsorption energy of Lithium in the rechargeable batteries.

^aShahid Chamran University, Golestan boulevard, Ahvaz, Khuzestan, Iran.

^bShahid Rajaee Teacher Training University, Lavizan, Tehran, Iran. E-mail:
j.beheshtian@srttu.edu

ARTICLE

Physical Chemistry Chemical Physics

This paper is organized as follows: In Sec. 2, we outline the computational method that we use. The results are presented in Sec. 3 and the related discussions follow afterward. Finally, we summarize our results and present our conclusion in Sec. 4.

2 Computational Methods

All our density functional theory (DFT) calculations were carried out within the generalized gradient approximations (GGA) for exchange-correlation energy term, as implemented in the Quantum-ESPRESSO package.²² The double numerical plus polarization (DNP) basis set and PBE functional²³ were adopted. Because of the weak interactions are not well described by the standard PBE functional, we adopted a PBE-D (D stands for dispersion) approach with the Grimme vdW correction. This approach is a hybrid semi empirical solution that introduces damped atom-pairwise dispersion correction of form C_6R^{-6} in the DFT formalism. The accuracy of the DNP basis set is comparable to that of People's 6-31G** basis set. The Brillouin zone (BZ) of the silicene supercell was sampled in k-space within Monkhorst-Pack scheme²⁴, where the convergence of total energy with respect to the number of k-points in BZ is carefully tested. Monkhorst-Pack Method is applied for the calculation of sums in Irreducible Brillouin Zone (IBZ). The structure optimization was symmetry unrestricted and was carried out using conjugate-gradient algorithm. The convergence criterion of self-consistent calculations for energy is chosen as 10^5 eV between two consecutive steps. For the adsorption of the Li and Li⁺ onto silicene surface, we use non-spin-polarized calculations. In all of the calculations, periodic boundary conditions are used within the supercell geometry, and the vacuum spacing between silicene layers in adjacent supercells is taken as 20 Å. For partial occupancies the Gaussian smearing method is used.

For the most stable lithiation patterns, the adsorption energy of lithium metal and lithium ion on the silicene surface was calculated using the following equation:

$$E_{ad} = (E_{Si} + nE_{Li} - E_{Si+Li})/n \quad (1)$$

Where E_{Si+Li} and E_{Si} are the total energies of silicene surface with and without Li adatoms, respectively, E_{Li} is the energy of atomic lithium or ionic lithium calculated with spin polarization, and n is the number of adsorbed Li atoms.

3 Results and discussion

To check our suggestion that silicene can replace with the graphene anode in Li batteries, we not only pay attention to the adsorption behavior of the lithium atoms onto silicene and graphene surface, but also look at the lithium storage capacity of these materials. Then, we calculated the energy barriers of silicene against Li/Li⁺ adsorption. At the end, we turn to test the lowest energy configurations obtained from these relaxations for checking the stability of Li covered silicene using DFT simulations.

3.1 The structure of the pristine silicene and graphene surface:

To illustrate the changes in the band topology of anode materials with and without Li adsorption, we simulate the relaxed structure of 2D silicene sheet (buckled, $\theta=101.7^\circ$), depicted in Figure 1 (b) which matches in the size with the graphene cell (Figure 1). As can see in Figures 2(a, b) the band structure of standalone silicene has first conduction band below the Fermi level, and therefore the DOS at this energy has a finite value, indicating that silicene is a semimetallic with 0.036eV band-gap. It has been predicted that the monolayer silicene and graphene have lattice parameters and bond lengths, which are in good agreement with experimental observation.²⁵⁻³¹

Silicene band gap is predicted to be zero like that observed in the graphene surface.³²⁻³³ In our calculations the usage of PBE approach leads to an underestimated band gap of 0.036eV.³⁴ We can note that our calculations of the band dispersions for monolayer silicene only exist for freestanding ones. Despite the experimental realizations of monolayer silicene grown on different substrates,³⁵⁻³⁹ (e.g. having an energy band gap of 0.210 eV³⁶) to date there has been no reports on existence of monolayer silicene in the free standing form which makes direct comparison of our band gap with experimental results somewhat risky.

3.2 Comparison between lithium adsorption over silicene and graphene

First, we have systematically studied the adsorption behavior of a Li metal atom on single-layer silicene (Li_1Si_{24}). Our results with a (11.69×13.32×20.00) supercell of silicene sheet are consistent with DFT calculations. Using larger supercells reduced the boundary effects and allowed for more degrees of freedom when exploring adsorption patterns, but has significantly increased computation time. Next, we investigate the adsorption of Li ion onto silicene sheet. At the end, we calculated the energy barrier against Li adsorption.

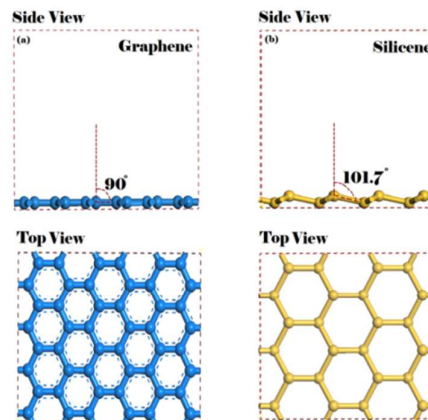


Figure 1. Top view and side view of atomic configuration of (a) graphene and (b) silicene optimized supercell. The blue balls represent C atoms and gold balls represent Si atoms. The buckling height of silicene at this configuration is $\Delta=0.448\text{\AA}$. The values of angle between neighboring atoms and the direction normal to the surface of silicene, $\theta=101.7^\circ$ calculated using GGA.

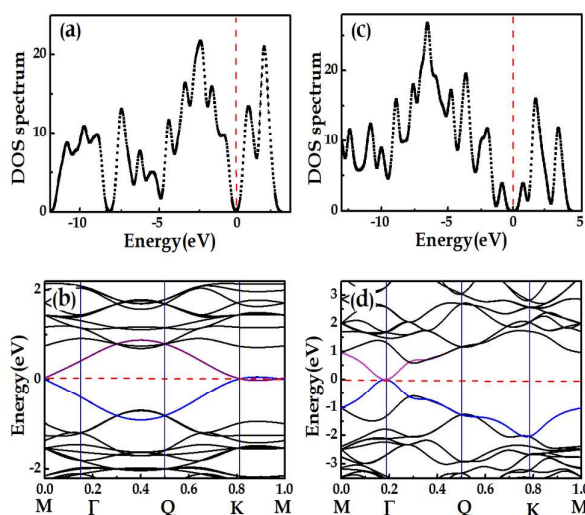


Figure 2. The corresponding density of state (DOS) and energy band structure of (a,b) silicene and (c,d) graphene in $(4 \times 4 \times 2)$ supercells. Fermi level is set to zero. DOS is broadened by Gaussian smearing with 0.14 eV.

3.2.1 The structure and stability of a single Li atom decorated silicene

The energy calculation is done by calculating the adsorption energy of system. A monkhorst pack mesh of $(4 \times 4 \times 2)$ special points is used for integration in reciprocal space. We began with one Li metal adsorption onto the silicene cell.

There are many possible sites for a Li-metal atom to occupy. Four non-equivalent adsorption sites (Figure 3) are investigated: the hollow site is right above the centre of a silicone hexagonal ring; the top site is above the higher Si atom; the valley site is above the lower Si atom; and the bridge site is above the middle of the Si-Si bond. The configurations tested include but are not limited to those shown in Figure 3.

Optimizations show that the Li atom adsorbed at the hollow site has highest energy with $E_{ad} = 3.09$ eV, while adsorption energy between Li atoms and silicene surface in two other configurations (T and V) lead to slightly weaker results with $E_{ad}=2.89$ eV.

When Li atom located at the bridge (B) site, it seems that under the adsorption process the Li atom is mobile and quickly moves on the silicene surface and preferably lies on the hollow sites. Therefore, a single Li atom prefers to be located at the H site of benzene ring rather than the other sites, which is in good agreement with the previous DFT calculations for preferable adsorption site on the silicene surface.⁴⁰

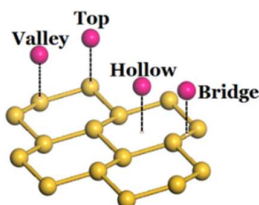


Figure 3. Preferable adsorption sites, valley, top, bridge and hollow on a silicene lattice. Here we do not consider all configurations and focus on the most stable adsorption energy. The dashed line denotes the equilibrium adsorption sites.

It is interesting to note that Li adsorption has little effect on the valence band edge and it changes the conduction band edge too. The energy gap for adsorption to H site is calculated to be 0.067 eV.

The adsorption energies of Li atoms which are interacting with silicene depend on the distance between Li and surface. When the distance between Li atom and silicene surface is enlarged to be 1.68 Å, adsorption energy of Li atom on H site is 3.09 eV.

Our calculations show that the adsorption of Li atom on silicene is strong and it is able to open a direct band gap at the Dirac point in silicene, ranging from 0.044 to 0.067 eV in different adsorption sites. This band gap is mainly induced by the sublattice symmetry breaking mechanism. The Li adsorption leads to a charge transfer from Li to Si atoms due to a large difference in electronegativity between Li and Si atoms which build a perpendicular electric field in silicene.

It has been established that this perpendicular electric field breaks the sublattice symmetry and thus opens a band gap in silicene. The asymmetry between two sublattices increases with the increasing coverage and the band gap is correspondingly increased.

As shown in Figures 4(c) and (d), the Li adsorption onto silicene enhances the electrical conductivity of silicene by modifying DOS peaks around Fermi energy and appearing additional peaks in DOS spectrum. The DOS of Li-silicene system near E_F have distinct change, so the conductivity change is observable.

By comparing Figures 2(d) and 4(d), one finds that for the Li-silicene, the number of the π^* -like bands crossing the Fermi level is greater by 1 than that for the silicene system, due to the increase of adsorbing. The bands near the Fermi level are mainly π^* -like bands derived from Si atoms, but the inner-sublayer and outer-sublayer Si atoms have slightly different contributions to the DOS. The Li-derived s-band is a wide band and its DOS below E_F is very low, indicating that electron occupation of this band is small.

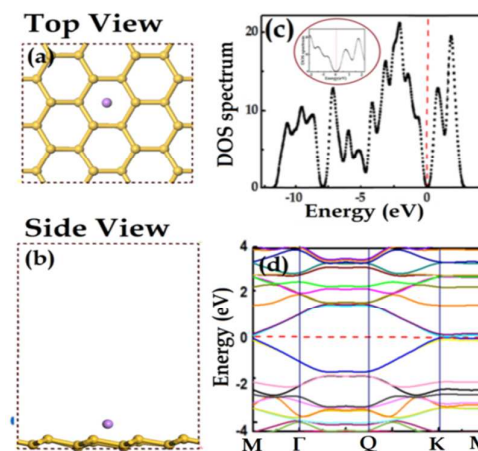


Figure 4. A single Li atom adsorbed onto the silicene supercell with $(4 \times 4 \times 2)$ special points, simulated in hexagonal box with dimensions $12 \times 13 \times 20$. (a) Top and (b) side view of the atomic configurations of the Li-atom adsorbed at the H-site of silicene above centre of hexagonal ring. Gold and orchid balls represent Si and Li atoms,

ARTICLE

Physical Chemistry Chemical Physics

respectively. (c) DOS spectrum of silicene doped with Li atom. The Fermi level is set to zero for the system including silicene. (d) Band structure of silicene doped with Li atom on top of the hollow site.

An analysis of the Mulliken atomic charges shows that the Mulliken charge transfer from Li to the silicene is about 0.25 electron for the H site. Our calculation indicates that the electrons of Li atoms are transferred into the inner-sublayer Si atoms rather than the outer-sublayer ones. Since the Li ions are positively charged and inner-sublayer Si atoms are negatively charged, the strong ionic bonding takes the place of weak vdW force in the silicene surface. The Mulliken charge calculation and adsorption energy between Li atom and silicene further indicate that the system of Li-silicene is a chemical adsorption.

For the Li-graphene systems the energy gap is closed and the Fermi level moves up into the conduction bands due to the increase of electron density, indicating that the Li adsorption makes graphene metallic. As shown in the Figure 5, after Li adsorption onto graphene surface DOS of graphene near Fermi level is increased, comparing with that of pristine graphene. When Li is adsorbed on the graphene, 0.46e charge transferred from Li to graphene results in the upshift of Fermi level. However, part of the charge still remains in the 2s orbital of Li. Silicene has larger dispersion in the K-M direction than that of the graphene. This means that is hard for electrons and holes to be transported across graphene layers, indicating the conductivity across silicene layers is more than that of the graphene layers. It is seen that our theoretical results for graphene are in good agreement with the experimental results.⁴¹⁻⁴⁴ Full of our theoretical results of adsorption onto graphene surface are not given in this paper for brevity.

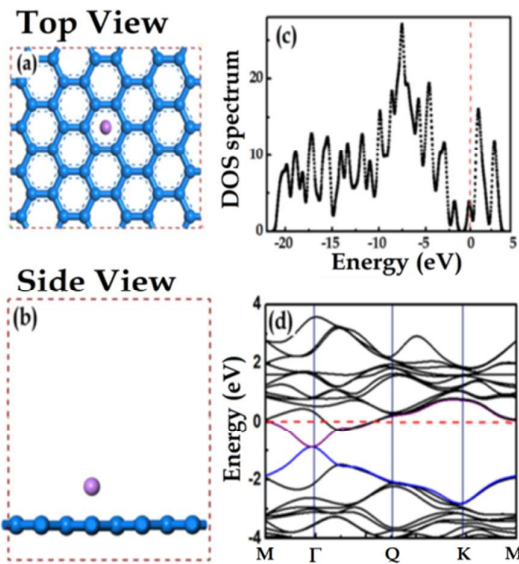


Figure 5. A single Li atom adsorbed onto the graphene supercell. (a) Top and (b) side view of the atomic configurations of the Li-atom adsorbed at the H-site of graphene above centre of hexagonal ring. Blue and orchid balls represent C and Li atoms, respectively. (c) DOS spectrum of graphene doped with Li atom. The Fermi level is set to zero for the system including graphene. (d) Band structure of graphene doped with Li atom on top of the hollow site.

3.2.2 The structure and stability of a single Li-ion decorated silicene

In this section, we introduce a lithium-ion adsorption onto the silicene surface. We have considered four different initial configurations although only introduced Li ion on top hollow sites of the benzene rings based on our finding by the same methods as discussed above. It was observed that during the adsorption process, Li^+ ions adsorbed in the centre of their closest benzene ring.

As can be seen from Figure 6, the effect of the considerably lower electronegativity and larger atomic radius of Li atom is observable in the calculated adsorption energy of Li^+ onto the surface in comparison to that of the Li atom. At the same distance from the silicene surface, the Li-metal ion adsorption energy (2.31eV) is smaller than the corresponding adsorption energy of Li-atom (3.09eV). So, there is a meaningful relationship between adsorption energy and Li charge. The more positive charge of Li^+ causes more tendency of Li ion to draw bonding electrons to itself. So the released energy of Li ion on the silicene surface is less than the released energy of Li atom on it.

3.2.3 The energy barrier against a Lithium atom/ion adsorption onto silicene

It is known that the rate performance of the electrode material is determined by the electrical conductivity and lithium diffusion characters. Understanding the diffusion of Li on materials is important because the charging times as well as the power density of a battery are related to the ability of Li atom/ion to migrate efficiently through electrolyte and electrodes. Thus the diffusion of lithium adatom on silicene surface is examined in our calculations.

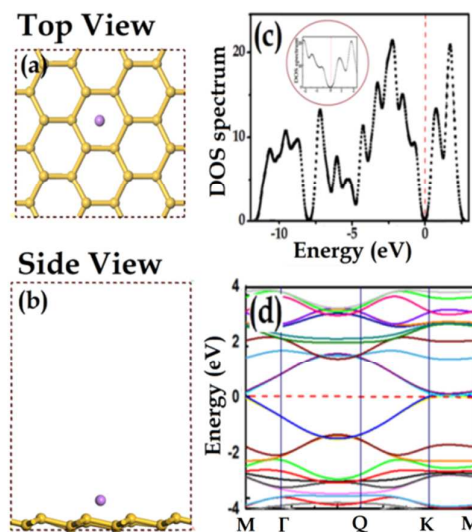


Figure 6. A single Li-ion adsorbed onto a supercell of silicene. (a) Top and (b) side view of the atomic configurations of the Li-ion adsorbed at the H-site of silicene above centre of hexagonal ring.(c) DOS spectrum of silicene doped with li. Gold and light orchid balls represent Si and Li atoms, respectively.

Due to the sensitivity of the adsorption energy to distance, varying the vertical distance between Li and silicene surface enables us to calculate the energy barrier of silicene. These barriers are calculated as the difference in energy for the maximum and minimum stable states in the hollow points along the diffusion path (Figure 7).

Optimized Li positions for these points are calculated by varying the Li atom distance to the silicene plane. It can be seen that with elongating (or shortening) of the vertical distances, the magnitude of total energy changes non-linearly with z. The minimum energy barrier to the migration of Li and Li^+ in this pathway revealed from the calculated energy landscape in Figure 7 to be 1.70 and 1.75 eV. These values are numerically smaller than the barrier in the case of the graphene sheet (7.40 -10.12 eV⁴⁵⁻⁴⁶) and for graphenylene (which is reported about 9.24 eV⁴⁷) due to the buckling of silicene. So silicene as an active material for storing Li shows higher performance than those of many reported for graphene-base anodes. Our energy barrier of a lithium atom through hexagonal ring for silicene is also smaller than the energy barrier for entry of Li atom from outside the tube 8.75-13.5 eV⁴⁵⁻⁴⁸. The energy barrier of Li atom adsorption onto silicene is higher by about 0.05 eV than that of Li ion. The major difference is the decreasing number of electrons as you go from Li to Li^+ . That causes greater attraction between Li and silicene surface. This confirms that Li atom is more favorable than the case of Li ion to adsorb onto silicene surface which is in good agreement with the more tendencies of Li ion to draw bonding electrons towards itself rather than the Li atom. Diffusion of a Li ion from one side to another one can occur via a hollow site by overcoming the energy barrier of ~1.75 eV. Hence, Li adatom can mobile between multilayer silicene in the lithium ion batteries. In an ideal situation, these results would imply that Li atom-silicene presents a faster discharge profile, and therefore a higher power density of the Li battery.

In the past works, theoretical study of the Li adsorption on carbonaceous materials in different paths presented.⁴⁴ The different calculated paths present different barrier profiles.⁴⁹ It appears that the most likely migration path on graphene surface is between subsequent hollow sites passing through the nearest valley site.⁴⁹ It features a zigzag path way.

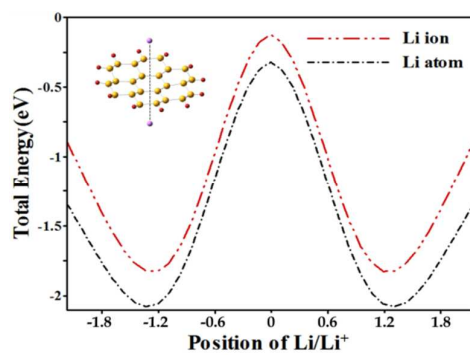


Figure 7. Energy variation of the Li/Li⁺ while it penetrates from upper side to the lower side of silicene. Zero in the x-axis indicates the position of silicene layer.

The calculated diffusion barrier for this path of a lithium adatom on the silicene surface is 0.14 eV which is lower than the lithium diffusion from a hollow site to a nearest neighboring one on perfect graphene (0.17 eV for same diffusion barrier). So the diffusion barrier for lithium migration on silicene decreases by about 0.3eV. This suggests that the rate performance can be better for silicene comparing to that of graphene for Li ion Storage. Our lithium diffusion barrier on silicene is also lower than the lithium diffusion barrier on the black phosphorus (0.16eV for diffusion barrier).⁵⁰

3.2.4 The structure and stability of a single Li-ion between bilayer silicene and graphene

There have been several reports on the different morphologies of bilayer silicene.⁵¹⁻⁵² In particular, a stable packing mode named AB morphology (Figure 8(a)) , in which silicon atoms in the upper layer are directly upon the top of centre of hollow sites of lower atoms. The cell parameters together with all atomic coordinates, were optimized for given configurations at both the presence and absence of Li. In the following, we optimized the geometry of structures that consist of two silicene layers stacked together in AB arrangement. We used this configuration to study the interaction of Li atom (ion) with the bilayer silicene. As can see in Figure 8, Li-bilayer silicene is a semimetal with a significant direct energy gap of 0.067eV. Linear dispersion bands at Dirac cone of bilayer silicene after Li adsorption become parabola-like. The intercalation of Li atoms expands the interlayer distance between silicene layers from 2.53 Å to 3.22 Å. The calculated adsorption energy between Li atom and bilayer silicene $E_{ad}=2.50\text{eV}$ is lower than that of the monolayer silicene (3.09eV). So in the next section we consider adsorption onto one layer to judge about monolayers. Mulliken charge transfer from Li ion to the bilayer silicene is ~0.46electron and that for monolayer silicene is calculated ~0.35electron.

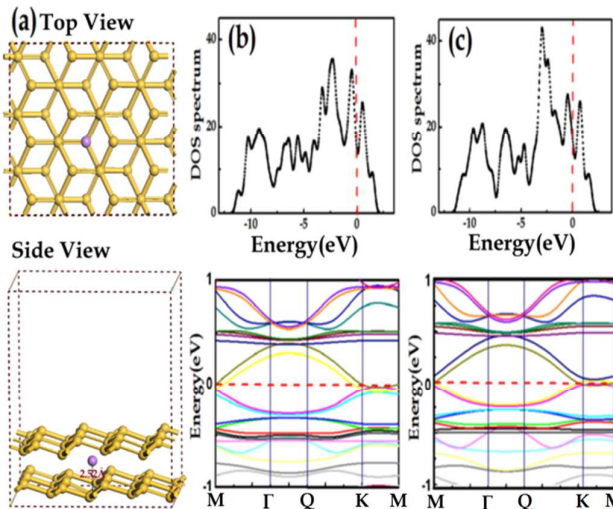


Figure 8. Top (upper) and Side (bottom) views of geometric structure of Li between silicene surfaces (a). DOS spectrum and band structure of Li atom (b) and Li ion (c) onto bilayer silicene.

ARTICLE

Physical Chemistry Chemical Physics

Similar to electronic properties of bilayer silicene, in the AB stacking bilayer graphene case is shown in Figure 9. The separation distance between the graphene layers in bilayer graphene is 3.748 Å, larger than that of graphite (3.34 Å)⁵³⁻⁵⁴ and agree well with previous experimental result (~3.75 Å).⁵⁵ Li adsorption causes an expansion in interlayer distance of graphene layer over a range up to 0.15 Å. In the lowest energy state, Li located close to a H site with 1.71 Å adsorption height and 2.19 Å far from T site of other graphene surface.

3.3 The structure and stability of Li-covered silicene supercell

The higher number of adsorbed Li on the silicene surface results in higher charge distributed on the surface. If a cluster has a larger Li charge, its sandwich structure will also have a larger Li charged. This suggestion could be used to avoid time consuming calculations which conclude the optimization for larger sandwich shape cases. So, we can consider single layers to judge about its sandwich structure charge storage capacity relative to another one.

We select Li-covered silicene as a representative for this purpose and show its electronic structure in Figure 10. In the 50.0% coverage, it was observed that during the absorption process, all Li atoms are adsorbed in the centre of their closest benzene ring, at the same distance from the silicene surface (1.73 Å). The distance of all lithium atoms from the silicene surface are equal with an accuracy of 10⁻² Å. Adsorption energy Li atom on silicene surface is 2.38 eV per Li. The Li-covered silicene does not undergo the deformation and the adsorbed Li atom remains at its stable state and does not diffuse to other site on silicene. Adsorption modifies the DOS around the Fermi energy and additional peaks appear in DOS spectrum. From the total DOS shown in Figure 10(c), one can see that the DOS at the Fermi level increases with adsorbing.

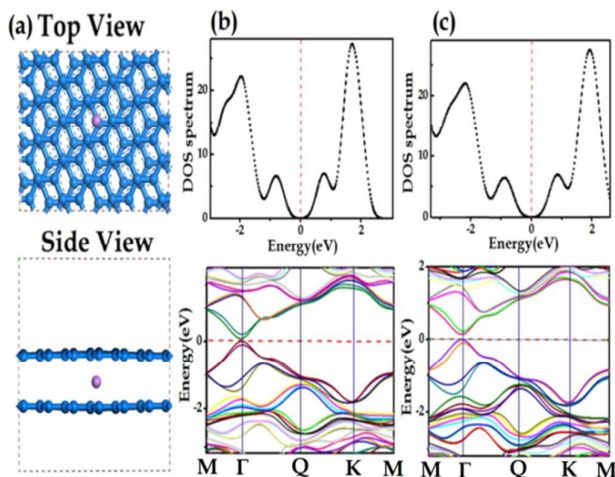


Figure 9. Top (upper) and Side (bottom) views of geometric structure of Li between graphene surfaces (a). DOS spectrum and band structure of Li atom (b) and Li ion (c) onto bilayer graphene

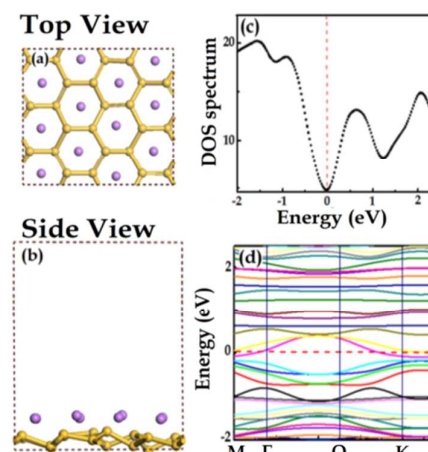


Figure 10. Silicene supercell with 50% Li coverage. (a) Top and b) side view of the atomic configurations of the Li atoms adsorbed at the H-sites of silicene above center of hexagonal rings. (c) DOS spectrum of silicene doped with 50% Li coverage. Gold and light orchid balls represent Si and Li atoms, respectively.

The investigated Li-covered silicene is not intrinsic semimetal, since its band gap is below the Fermi level. As shown in Figure 10. In the Li-covered silicene band structure a band gap of about 0.23 eV opened between the π and π^* band at the Dirac point due to the more Li adsorbing. The band structure exhibits a Dirac point roughly 0.67 eV below E_F .

We have repeated our calculations by use of the same graphene cell which has 50% Li atoms on its surface. When 50% Li atoms are located onto the graphene, it will bend. More calculations show that the graphene under investigation has limited Li storage capacity and low surface area than the same silicene surface. Figure 11, where 18 and 10% Li adsorption ratios structures are taken as examples, shows that in comparison to silicene cell in the same condition this structure store Li charge about 90% less and the distortion of graphene structure is not negligible.

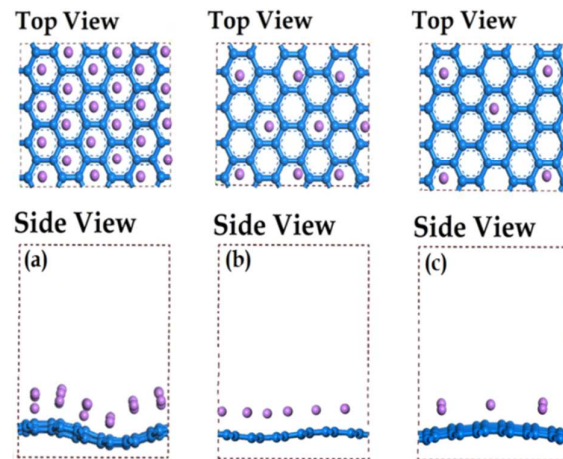


Figure 11. Schematics of partial Lithium adsorption configurations for 50% (a), 18% (b) and 10% (c) adsorption ratios on a 48-carbon-atom supercell. Upper panels show top views and bottom ones show side view of the structures.

According to above results, this capability gives silicene a greater theoretically capacity of simple storage and good performance than the graphene anode. Using the silicene anode shorts the charge time of batteries and achieve higher-energy density by store more number of adsorbed Li in the same silicene surface than the graphene anode. So, it seems a good suggestion to use silicene layer for adsorb a higher number of Li atoms and improve the performance of Li-batteries.

4 Conclusions

The preferred sites for adsorption onto silicene and graphene surface were explored by testing various lithiation configurations on these two supercell models. Li adsorption modifies the DOS around the Fermi energy and additional peaks appear in DOS spectrum. Adsorption turns silicene into a narrow gap semiconductor. We also predict the maximum energy barrier for the migration of Li/Li⁺ adatom on silicene sides is only 1.70/1.75 eV. Low energy barrier implies that Li adatoms can easily penetrate into bilayer or multilayer silicene. Because of more charge storage capability and better energy density of silicene than the graphene surface, using the silicene as anode material has the potential of increasing the performance of LiBs. Silicene could serve as high-capacity host of Li in LiBs. Lithium adsorption onto silicene is still not understood fully because of the lack of reliable experimental methods to make free standing silicene so far. This makes the theoretical evaluation of Li adsorption important and it will be interesting to compare our results with future experiments. Since our models are in good agreement with previous predictions, this study proposes to create better anode material for LiBs one can use silicene as anode with higher Li⁺ storage capacity than the graphene.

References

- N. Imanishi, A. C. Luntz and P. G. Bruce, New York: Springer-Verlag, 2014, 318.
- J. M. Tarascon and M. Armand, *Nature*, 2001, **414**, 359-67.
- P. Lian, X. Zhu, S. Liang, Z. Li, W. Yang and H. Wang, *Electrochim Acta*, 2010, **55**, 3909-14.
- K. Sato, M. Noguchi, A. Demachi, N. Oki and M. Endo, *Science*, 1994, **264**, 556-8.
- J. M. Tarascon and M. Armand, *Nature*, 2001, **414**, 359-367.
- J. Zhu, C. Gladden, N. Liu, Y. Cui and X. Zhang, *Phys. Chem. Chem. Phys.*, 2013, **15**, 440-443.
- Y. Yao, M. T. McDowell, I. Ryu, H. Wu, N. Liu, L. B. Hu, W. D. Nix and Y. Cui, *Nano Lett.* 2011, **11**, 2949-2954.
- J. I. Lee, J. H. Park, S. Y. Lee and S. Park, *Phys. Chem. Chem. Phys.*, 2013, **15**, 7045-7049.
- C. K. Chan, H. Peng, G. Liu, K. M. Wrath, X. F. Zhang, R. A. Huggins and Y. Cui, *Nat. Nanotechnol.*, 2008, **3**, 31-35.
- U. Kasavajjula, C. Wang, and A. John Appleby, *J. Power Sources*, 2007, **163**, 1003-1039
- S. M. Seyed-talebi, M. Neek-amal, *J. Appl. Phys.*, 2014, **116**, 153507-7
- S. M. Seyed-talebi, J. Beheshtian, M. Neek-amal, *Appl. Phys.*, 2013, 124307-124307-7
- D. Pan, S. Wang, B. Zhao, M. Wu, H. Zhang, Y. Wang and Z. Jiao, *Chem. Mater.*, 2009, **21**, 3136-3142
- C. Wang, D. Li, C. O. Too and G. G. Wallace, *Chem. Mater.*, 2009, **21**, 2604-2606
- E. Yoo, J. Kim, E. Hosono, H. S. Zhou, T. Kudo and I. Honma, *Nano Lett.*, 2008, **8**, 2277-82
- M. Liang and L. Zhi, *J. Mater. Chem.*, 2009, **19**, 5871-5878
- Z. S. Wu, W. Ren, L. Xu, F. Li and H. M. Cheng, *ACS Nano*, 2011, **5**, 5463-5471
- A. L. M. Reddy, A. Srivastava, S. R. Gowda, H. Gullapalli, M. Dubey, and P. M. Ajavan, *ACS Nano*, 2010, **4**, 6337-6342
- Y.-X. Yu, *Phys. Chem. Chem. Phys.*, 2013, **15**, 16819-16827
- Y.-X. Yu, *J. Mater. Chem. A*, 2014, **2**, 8910-8917
- Y.-X. Yu, *ACS Appl. Mater. Interfaces*, 2014, **6**, 16267-16275
- P. Giannozzi, S. Baroni, N. Bonini, M. Calandra, R. Car, C. Cavazzoni, D. Ceresoli, G. L. Chiarotti, M. Cococcioni, I. Dabo, A. D. Corso, S. D. Gironcoli, S. Fabris, G. Fratesi, R. Gebauer, U. Gerstmann, C. Gougoussis, A. Kokalj, M. Lazzeri, L. M. Samos, N. Marzari, F. Mauri, R. Mazzarello, S. Paolini, A. Pasquarello, L. Paulatto, C. Sbraccia, S. Scandolo, G. Scalauzero, A. P. Seitsonen, A. Smogunov, P. Umari and R. M. Wentzcovitch, *J. Phys. Condens. Matter*, 2009, **21**, 395502.
- J. P. Perdew, K. Burke and M. Ernzerhof, *Phys. Rev. Lett.* 1996, **77**, 3865-3868.
- H. J. Monkhorst and J. D. Pack, *Phys. Rev. B*, 1976, **13**, 5188-5192.
- T. Botari, E. Perim, P. A. S. Autreto, A. C. T. van Duin, R. Paupitz and D. S. Galvao, *Phys. Chem. Chem. Phys.*, 2014, **16**, 19417.
- S. Yoshihiro, M. Ushio, S. Suzuki, *Bull. Chem. Soc. Jpn.*, 1988, **61**, 1577-1585.
- K. J. Koski and Y. Cui, *ACS Nano*, 2013, **7**, 3739-3743.
- S. Cahangirov, M. Topsakal, E. Aktürk, H. Şahin and S. Ciraci, *Phys. Rev. Lett.*, 2009, **102**, 236804.
- A. Kara, H. Enriquez, A.P. Seitsonen, L.C. Lew Yan Voon, S. Vizzini, B. Aufray and H. Oughaddou, *Surf. sci. Rep.*, 2012, **67**, 1-18.
- E. Scalise, M. Houssa, G. Pourtois, B. vander Broek, V. Afanas'ev and A. Stesmans, *Nano Res.*, 2013, **6**, 19-28.
- B. Feng, Z. Ding, S. Meng, Y. Yao, X. He, P. Cheng, L. Chen and K. Wu, *Nano letters*, 2012, **12**, 3507-3511.
- M. Neek-Amal, A. Sadeghi, G. R. Berdiyorov, and F. M. Peeters, *Appl. Phys. Lett.*, 2013, **103**, 261904
- Q. Ru-Ge, W. yang-Yang, and L. Jin, *Chin. Phys. B*, 2015, **24**, 088105
- H. Xiao, J. Tahir-Kheli, and W. A. Goddard, *J. Phys. Chem. Lett.*, 2011, **2**, 212-217
- B. Aufray, A. Kara, S. Vizzini, H. Oughaddou, C. Leandri, B. Ealet, and G. Le Lay, *Appl. Phys. Lett.*, 2010, **96**, 183102-183103
- L. Tao, E. Cinquanta, D. Chiappe, C. Grazianetti, M. Fanciulli, M. Dubey, A. Molle and D. Akinwande, *Nat. Nanotech.*, 2015, **10**, 227-231
- A. Fleurence, Y. Yoshida, C. -C. Lee, T. Ozaki, Y. Yamada-Takamura, and Y. Hasegawa, *Appl. Phys. Lett.*, 2014, **104**, 021605
- M. Hossa, A. Dimoulas, and A. Molle, *J. Phys. Condens. Matter*, 2015, **27**, 253002
- P. Vogt, P. De Padova, C. Quaresima, J. Avila, E. Frantzeskakis, M. C. Asensio, A. Resta, B. Ealet, and G. Le Lay, *Phys. Rev. Lett.*, 2012, **108**, 155501
- H. Sahin and F. M. Peeters, *Phys. Rev. B*, 2013, **87**, 085423.
- L. J. Zhou, Z. F. Hou and L. M. Wu, *J. Phys. Chem. C*, 2012, **116**, 21780-21787.
- G. A. Tritsaris, E. Kaxiras, S. Meng and E. Wang, *Nano. Lett.*, 2013, **13**, 2258-2263.
- J. Hou, Y. Shao, M.W. Ellis, R.B. Moore and B. Yi, *Phys. Chem. Chem. Phys.*, 2011, **13**, 15384-15402.
- X. Fan, W. T. Zheng and J. L. Kuo, *ACS. Appl. Mater. Interfaces*, 2012, **4**, 2432-2438.

ARTICLE

Physical Chemistry Chemical Physics

- 45 K. Nishidate and M. Hasegawa, *Phys. Rev. B*, 2005, **71**, 245418.
- 46 M. Khantha, N. A. Cordero, J. A. Alonso, M. Cawkwell and L. A. Girifalco, *Phys. Rev. B*, 2008, **78**, 115430-9
- 47 Y.-X. Yu, *J. Mater. Chem. A*, 2013, **1**, 13559-13566
- 48 V. Meunier, J. Kephart, C. Roland, and J. Bernholc, *Phys. Rev. Lett.*, 2002, **88**, 075506
- 49 C. Uthaisar and V. Barone, *Nano. Lett.*, 2010, **10**, 2838-2842.
- 50 C. Henkel, S. Abermann, O. Bethge, G. Pozzovivo, S. Puchner, H. Hutter and E. Bertagnolli, *J. Electrochem. Soc.*, 2010, **157**, 815-820.
- 51 H. Fu, J. Zhang, Z. Ding, H. Li, and S. Meng, *Appl. Phys. Lett.*, 2014, **104**, 131904.
- 52 S. S. Cahangirov, M. Topsakal, E. Akturk, H. sahin, and S. Ciraci, *Phys. Rev. Lett.*, 2009, **102**, 236804.
- 53 C. Y. Wang, D. Li, C. O. Too and G. G. Wallace, *Chem. Mater.*, 2009, **21**(13), 2604-2606.
- 54 A. Abouimrane, O. C. Compton, K. Amine and S. T. Nguyen, *J. Phys. Chem. C*, 2010, **114**, 12800–12804.
- 55 J. Hou, Y. Shao, M. W. Ellis, R. B. Moore and B. Yi, *Phys. Chem. Chem. Phys.*, 2011, **13**, 15384-15402.